Finite Element Analysis of the Tunnel-Beneath Piled Building Interaction

Thai Ngoc DO*, Anatoliy Grigorevich PROTOSENYA, Nikita Andreevich BELYAKOV, Vi Van PHAM, Quang Van NGUYEN

Abstract: The growth of cities induced an increased demand for infrastructure including tunnel constructions. Because the urban ground usually is soft soil therefore tunnel constructions may cause ground settlement and damage the structures around. So, it is very important to carefully consider the tunnel construction effect on the design, construction, operation, and risk assessment of structures around the tunnel. In this paper, the finite element method was used to study the influence of the tunnel excavation on beneath piled buildings at the Hanoi metro line 03. These results indicate that the internal forces and displacements of the pile are greatest for the front pile closest to the tunnel in the group, which is the first pile to be loaded in the group. Two parameters: the tunnel burial depth and the distance from the tunnel centreline to the beneath-piled building have been investigated. These results found that the distance from the tunnel axis to the beneath piled building increases, while both the internal forces and displacements of the pile decrease. These internal forces and displacements increase with greater tunnel burial depth. The magnitude of normal forces and bending moments in the tunnel lining increase as the tunnel burial depth increases, while normal forces increase and bending moments in the tunnel lining decrease when the distance from the tunnel axis to the beneath-piled building decreases.

Keywords: finite element method; piled building; tunnel; underground construction

1 INTRODUCTION

The twin tunnels constructions in the soft ground cause ground movements [1, 2]. These ground movements may significantly affect the structures beneath and must be considered in the planning process. The tunnel's influence on beneath-piled buildings has been reported [3-11]. These studies have shown that the effect of tunnelling on beneath-piled building response depends on many factors such as building characteristics, pile length, construction method type, and soil properties. The influence of building stiffness and geometries on the behaviour of the building has been investigated by finite element analyses. O'Reilly & New (1982) reported that the surface soil displacement is in the transverse direction and the displacement vectors are towards the centreline of the tunnel [12]. Attewell & Woodman (1982) indicated that the longitudinal settlement profile can be derived by considering a tunnel as a number of point sources in the longitudinal direction and by superimposing the settlement craters caused by each point source [13]. Mair et al. (1996) reported the ground movements during the excavation of a new escalator tunnel from the basement of a piled building in London [14]. Considering the effects of the building self-weight on tunnelling induced ground movements and building deformation was identified by Franziu et al. (2004) [11]. The effect of tunnel location on the tunnel-pile interactions has been proposed by Marshall et al. (2015) [15]. Franza and Marshall (2018) reported the effects of structural stiffness and weight on maximum settlements above the tunnel [16]. The presence of piled building close to the tunnel which is under construction leads to the unsymmetrical inhomogeneous medium surrounding the tunnel. Depending on the distances from the piled building to the tunnel in both vertical and horizontal directions, the interaction between piled building and tunnel will be varied [17-19]. In this paper, the finite element method was used to analyse the influence of the tunnel construction on the beneath-piled building, the case of the Hanoi metro line 03. The Hanoi metro line 03 is constructed in the urban area with a varying tunnel burial depth and variable distance from the tunnel centreline to the beneath piled building.

Both the tunnel burial depth and the distance from the tunnel centreline to the beneath-piled building have a great influence on ground movements, both horizontal and vertical. These two parameters also have a significant influence on the internal forces and displacements within both the piled building and tunnel lining, so it is necessary to investigate the influence of these two parameters on the interaction between the tunnel and beneath-piled building. The effect parameters have been investigated, including the tunnel burial depth and the horizontal distance from the tunnel centreline to the beneath-piled building. The internal forces in the tunnel lining and lateral deflection, vertical movement, the normal force, and the bending moment of the piles are considered.

2 TUNNEL CONSTRUCTION EFFECTS ON BUILDING DEFORMATION
2.1 Ground Surface Settlement Trough Caused by Tunnelling

Ground movements are caused by tunnel constructions in soft ground [20-23]. Fig. 1 illustrates the calculation diagram of surface settlement caused by tunnel construction under green-field conditions, without the presence of any other. The ground surface settlement trough can be well described by a Gaussian curve and can be expressed as follows [20]:

$$S = S_{\max} \cdot \exp\left(\frac{-x^2}{2i^2}\right) \qquad (1)$$

where: S is the surface settlement; $S_{\max}$ is the maximum settlement on the tunnel centreline; x is the distance from the tunnel centreline; i is the trough width parameter.
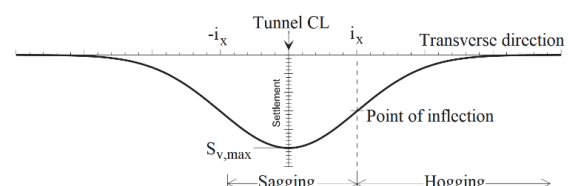

Figure 1 Green-field surface settlement trough [20]

2.2 Tunnel Construction Effects on Building Deformation

Addenbrooke et al., (1997) presented an approach that considers the building's stiffness when predicting tunnel induced building deformation [3] where the bending stiffness (EI) and axial stiffness (EA) are represented for the structure stiffness. While Parameter (B) represents the width size of the building model, the tunnel depth (z_0) and the eccentricity (e) is the centre distance between the building and the tunnel (Fig. 2).
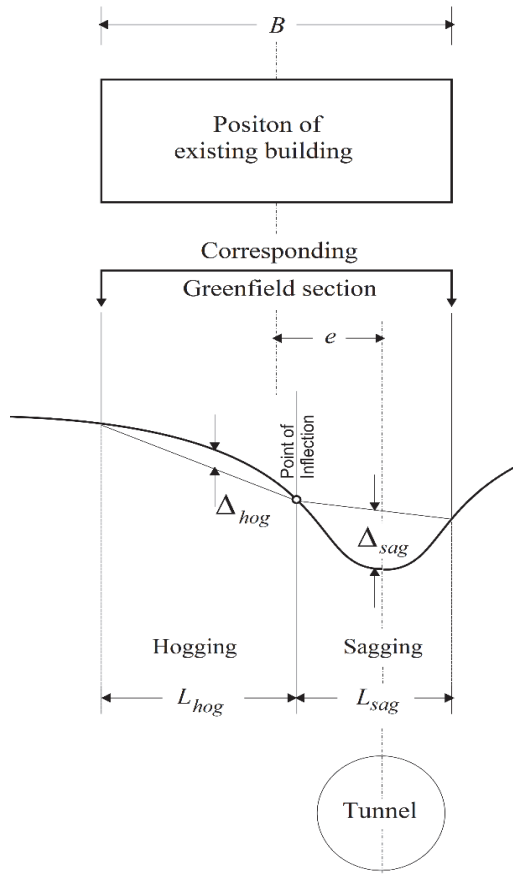

Figure 2 Geometry of the problem and definition of deflection ratio [3]

The stiffness of the building was related to that of the soil by determining the relative stiffness expressions:

$$\rho^* = \frac{EI}{E_s \left(\frac{B}{2}\right)^4}; \quad \alpha^* = \frac{EA}{E_s \left(\frac{B}{2}\right)} \qquad (2)$$

where E_S is the secant stiffness of the soil; ρ^* is referred to as relative bending stiffness whereas α^* describes the relative axial stiffness. The building deformation caused by the tunnel was determined by the deflection ratio DR and maximum horizontal strain ε_h. Addenbrooke et al. (1997) proposed to estimate building deformations by the modification factor; the design curves for modification factors in Fig. 3a and Fig. 3b are used to estimate the modification factors of sagging and hogging deflection ratio (M^{DRsag}, M^{DRhog}) and modification factors of maximum tensile and compressive horizontal strains: ($M^{\varepsilon ht}$, $M^{\varepsilon hc}$) The building deformation can be determined by multiplying the maximum deflection ratio for sagging and hogging zones in the greenfield deformation with the corresponding modification factors:

$$DR_{sag} = M^{DRsag} \cdot DR_{sag}^{GF}; \quad DR_{hog} = M^{DRhog} \cdot DR_{hog}^{GF} \qquad (3)$$

$$\varepsilon_{hc} = M^{\varepsilon hc} \cdot \varepsilon_{hc}^{GF}; \quad \varepsilon_{ht} = M^{\varepsilon ht} \cdot \varepsilon_{ht}^{GF} \qquad (4)$$

where DR_{sag} and DR_{hog} are the maximum deflection ratio for sagging and hogging zones, DR_{sag}^{GF} and DR_{hog}^{GF} are the maximum deflection ratio for sagging and hogging zones in the greenfield condition (with no building present), ε_{hc} and ε_{ht} are the maximum horizontal compressive and tensile building strains, ε_{hc}^{GF} and ε_{ht}^{GF} the maximum greenfield horizontal compressive and tensile building strains.

(a) modification factors of deflection ratio
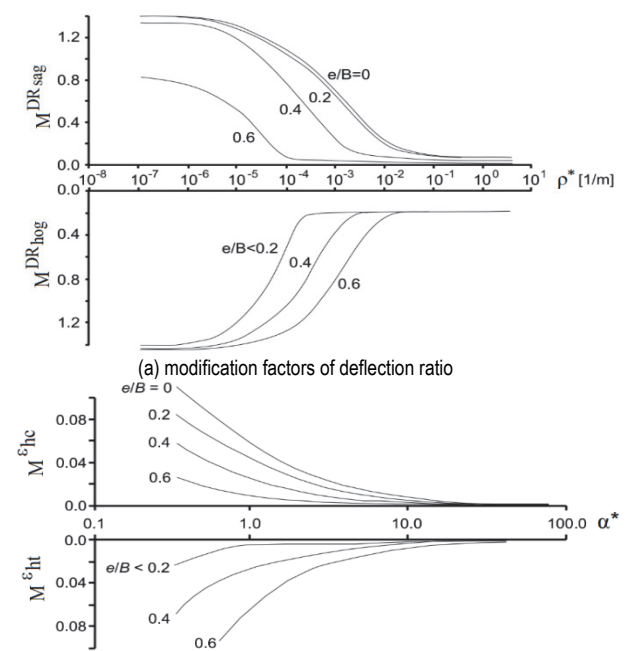
(b) modification factors of maximum horizontal strain
Figure 3 Design curves for modification factors [3]

3 FINITE ELEMENT MODELLING
3.1 Input Parameters

The development of infrastructure is a requirement to support the growth of major cities, including Hanoi, the capital of Vietnam. The first metro in Hanoi, Vietnam, is Project Metro line 03 of the Hanoi Metro Rail System. The tunnel is 4 km long, 6.3 m in diameter and located at the burial depths from 15 m to 35 m [24]. The Hanoi Metro line 03 was constructed in soft ground using a TBM machine and the parameters properties of the soil layers are presented in Tab. 1 [25]. The tunnel is excavated beneath the building and underground structures. These existing structures may be damaged by the tunnel construction. The geometry of the tunnel, piles, and soils shown in Fig. 4, was adopted [26]. In this study, the FEM method was used for analysis of the soil-piled building interaction. The effect parameters such as distance between the tunnel centreline and the beneath piled building (L), the tunnel burial depth

(Z) on the normal forces, bending moment of the tunnel lining and lateral deflection, vertical movement, the axial forces, and bending moment of the piles were investigated (Fig. 4). The numerical model was simulated using the plain strain FEM model (Plaxis 2D V20). The model comprised five soil types, and the soil properties are presented in Tab. 1. The dimensions of the model built in the FEM are 200 m in width and 75 m in height. The model includes 88954 nodes and 10837 elements, as shown in Fig. 5.
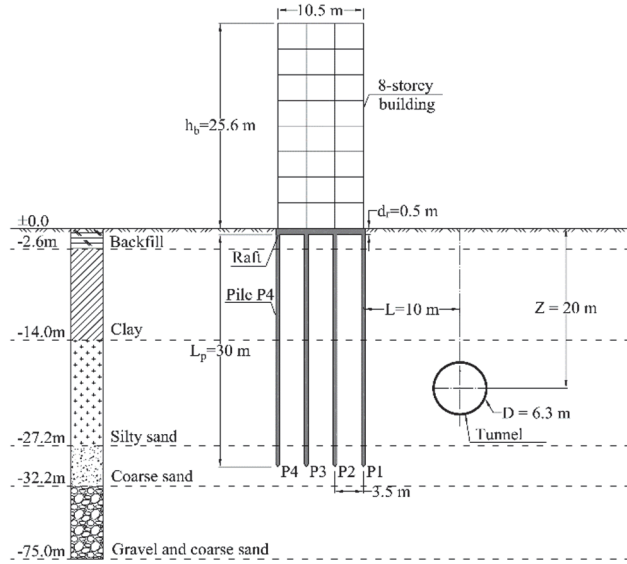

Figure 4 The soil, tunnel and piled structure geometries [26]

Table 1 Material parameters for the soil layers [25]

Parameter	Backfill	Clay	Silty sand	Coarse sand	Gravel and coarse sand
Thick layer / m	2.6	11.4	13.2	5.0	42.8
Dry weight, γ_{unsat} / kN/m³	18.5	19.5	20.0	20.5	21.0
Secant stiffness from drained triaxial test, E_{50}^{ref} / kN/m²	18500	21750	32650	45150	75450
Tangent stiffness for primary oedometer loading, E_{oed}^{ref} / kN/m²	18500	21750	32650	45150	75450
Unloading/ reloading stiffness, E_{ur}^{ref} / kN/m²	55500	65250	97950	135500	226400
Initial void ratio, e_{init}	0.5	0.5	0.5	0.5	0.5
Exponential power / m	0.5	0.5	0.5	0.5	0.5
Unloading/reloading Poisson's ratio, v_{ur}	0.2	0.2	0.2	0.2	0.2
Friction angle, φ / ⁰	28	25	25	34	35
Dilatancy angle, ψ / ⁰	0	0	0	1	1
Cohesion, c_{ref} / kPa	9.6	10	25	0.5	0.5
Interface strength reduction, R_{inter}	0.67	0.5	0.67	0.67	0.67

Table 2 Material parameters for the piled building [26]

Input Parameter	Tunnel lining	Raft	Building
Material type	Elastic	Elastic	Elastic
Isotropic	Yes	Yes	Yes
Axial stiffness, EA / kN/m	10.5×10^6	15×10^6	12×10^6
Bending stiffness, EI / kN·m²/m	7.875×10^4	312.5×10^3	16×10^4
Weight, w / kN/m/m	7.5	24	9.6
Poisson'ratio, v	0.15	0.15	0.15
Prevent punching	No	No	No

Table 3 Material parameters for the embedded piles [26]

Input Parameter	Unit	Pile
Material type	-	Elastic
Young's module, E	MPa	35×10^6
Unit weight, γ	kN/m³	24
Beam type	-	Predefined
Predefined beam type	-	Massive circular beam
Diameter, d	m	0.4
Pile spacing, $L_{spacing}$	m	3.5
Axial skin resistance	-	Linear
Skin resistance at the top, $T_{skin, start, max}$	kN/m	1.0
Skin resistance at the bottom, $T_{skin, sand, max}$	kN/m	100
Lateral resistance	-	Unlimited
Base resistance, F_{max}	kN	100
Interface stiffness factors, default values	-	Yes

During the static analysis, the top of the model is free, the model is assumed to be fully fixed at its bottom and the vertical sides of the model were fixed in the horizontal direction. The elements were present in the model: 15-node elements for the clusters, plate elements for the tunnel lining, raft and building, embedded piles row elements for the pile, and the soil-structural interface were adopted Fig. 5. The tunnel included into the analyses was $D = 6.3$ m in diameter with a tunnel depth of $Z = 20$ m. The building is 10.5 m wide and 8-storey structure. This foundation was a piled raft, each pile of diameter $d = 0.4$ m, pile length $L_p = 30$ m, the pile spacing was 3.5 m, and these piles were capped by a reinforced concrete raft 0.5 m in thickness as shown in Fig. 4. It should be noted that Hardening soil (HS) constitutive model is used. The tunnel lining, raft, and building properties are presented in Tab. 2 and the pile parameters in Tab. 3 are adopted. The numerical modelling was performed through the following steps:
- Defining the circumferential area of soil around the tunnel and building.
- Selecting an appropriate constitutive model and determining the required parameters.
- Applying the boundary conditions.
- In the phase, activation of the building.
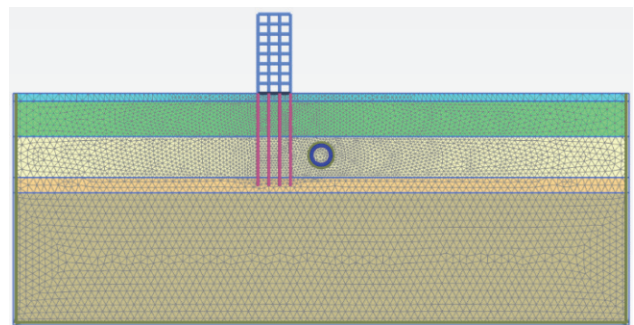- Construction of tunnel.

Figure 5 2D finite element model for the analysis of tunnel-soil-building interaction

3.2 Result of Calculation

The finite element model for the analysis of tunnel-soil-building interaction is shown in Fig. 5. This method has been used for the investigation of tunnelling-induced green-field settlement and the response of the piled building to tunnelling. The shape of the ground surface

settlement trough obtained by finite element analyses can be seen in Fig.6, the magnitude of maximum ground settlement at the surface has increased by 45% compared to the green-field settlement profile (17.0 mm to 30.2 mm), its position is displaced 10m towards beneath piled building. The maximum horizontal displacement (5.6 mm) has increased by 2% compared to the green-field value (5.1 mm), as shown in Fig. 7.
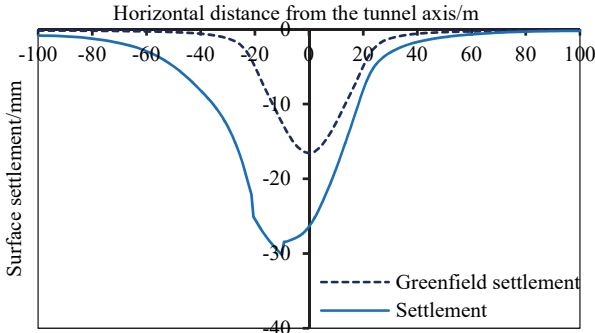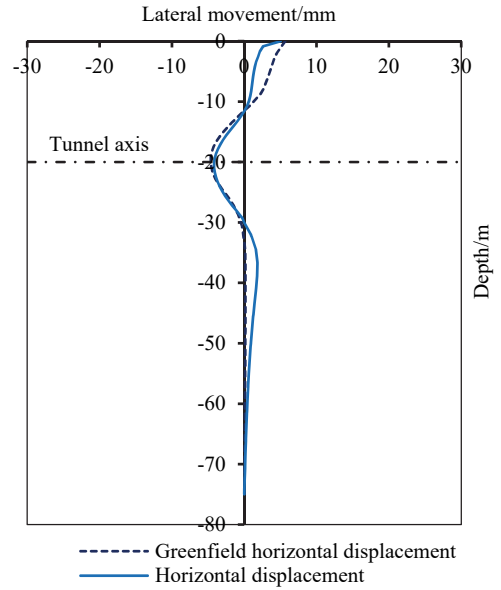
Figure 6 Ground surface settlement trough

Figure 7 Horizontal ground displacement, l = 1 0m away from the tunnel centreline
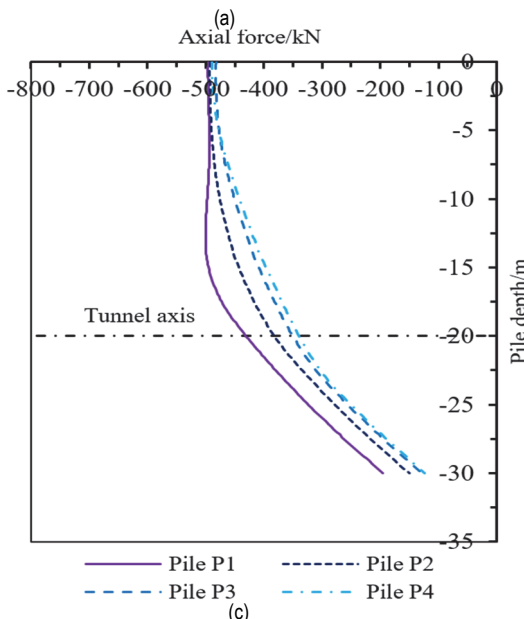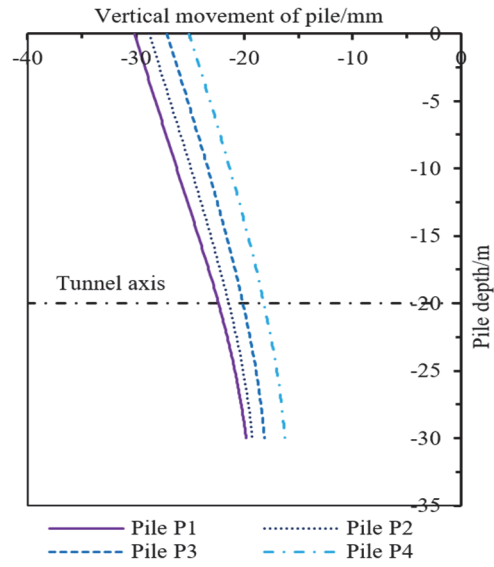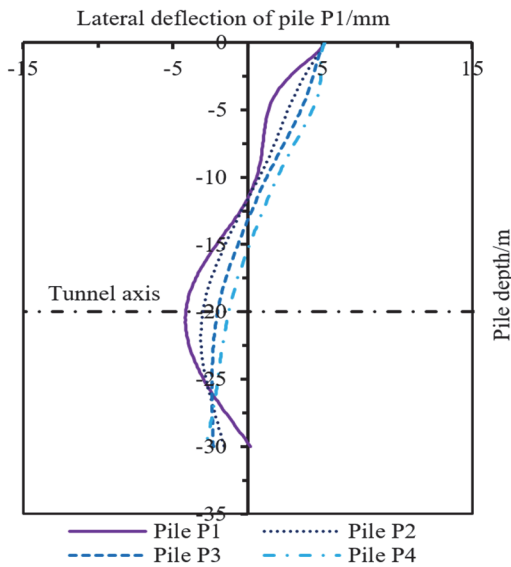
(a)

(b)

(c)

(d)
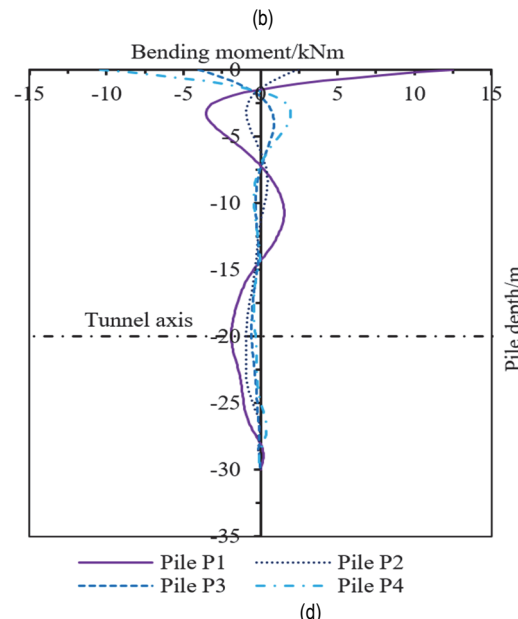
Figure 8 Distribution of (a) lateral deflection, (b) vertical movement, (c) axial force and (d) bending moment of piles

Fig. 8 shows the distribution of pile response profiles for lateral deflection, vertical movement, axial force, and bending moment of piles. The magnitude lateral deflection U_x of pile $P1$ occurring at the horizontal axis of the tunnel, located at a depth of 20 m was found to be 4.14 mm, whereas the value of U_x for $P2$, $P3$ and $P4$ were found to be 3.01 mm, 2.02 mm and 1.26 mm respectively. The maximum vertical movement U_{ymax} of the pile $P1$ was found to be 30.17 mm. The maximum vertical movement U_{ymax} can be seen to decrease to 28.81 mm, 27.14 mm and 25.10 mm for the pile $P2$, pile $P3$ and pile $P4$ respectively.

The magnitudes of the axial force occur at the horizontal axis of the tunnel, located at a depth of 20 m of $P1$, $P2$, $P3$ and $P4$ were found to be 430.18 kN, 381.78 kN, 350.09 kN and 339.42 kN respectively. Fig. 8d shows that the bending moment distribution of $P1$ is similar to the bending moment distribution of pile $P2$ and the bending moment magnitude of $P1$ is larger than that for pile $P2$. The bending moment distribution of pile $P4$ is similar to the bending moment distribution of pile $P3$ and the bending moment magnitude of pile $P4$ is larger than that of pile $P3$.
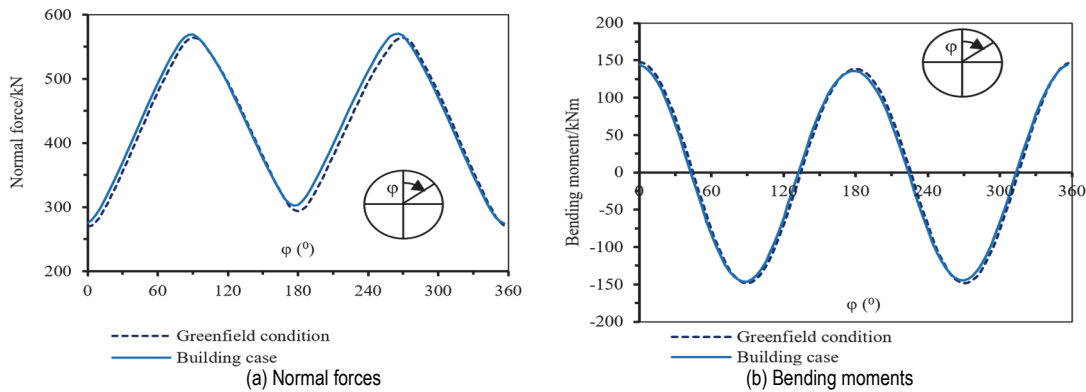

(a) Normal forces

(b) Bending moments

Figure 9 The internal forces in the tunnel lining
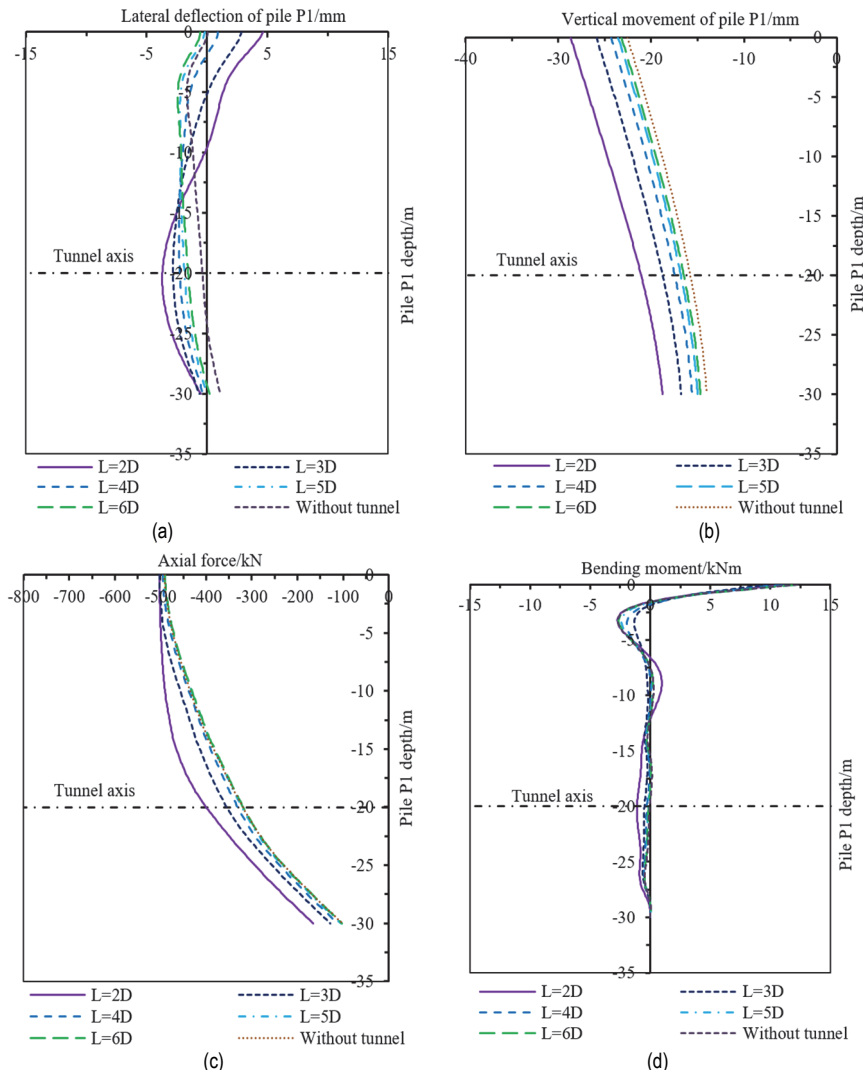

(a)

(b)

(c)

(d)

Figure 10 Distribution of (a) lateral deflection, (b) vertical movement, (c) axial force and (d) bending moment of pile P1 with varying distances from tunnel centreline to the beneath piled building L

Fig. 9a and Fig. 9b illustrate the distribution of axial forces and bending moments of the tunnel lining obtained by numerical analyses. The magnitude of maximum normal forces in the tunnel lining has increased by 1.1% compared to the green-field case (563.9 kN to 570.0 kN). The maximum bending moment in the tunnel lining has decreased by 1.5% compared to the green-field case (148.5 kNm to 146.3 kNm), as shown in Fig. 9b. The different responses of piles due to tunnelling are analysed. These results indicate that the magnitude of the pile $P1$ response is greatest, pile $P1$ is the first pile loaded in the beneath-piled building. The effect of the horizontal distance from the tunnel centreline to the beneath-piled building (L) and the tunnel burial depth (Z) on the response of pile $P1$ due to tunnelling were investigated from the finite element method and can be seen in Fig. 10 to Fig. 15.

The effect of the horizontal distance from the tunnel centreline to the beneath-piled building (L) on responses of the pile $P1$ is shown in Fig. 10. In this study, a range of distances from the tunnel centreline to the beneath-piled building was considered (2D, 3D, 4D, 5D and 6D) while keeping the depth of tunnel $Z = 20$ m and the other parameters presented in Tab. 1 and Tab. 2 are adopted. Fig. 10a and Fig. 10b illustrated the lateral deflection and vertical movement of pile $P1$ with a varying horizontal distance from the tunnel centreline to the beneath piled building of 2D, 3D, 4D, 5D, and 6D. These results found that lateral deflection and vertical movement of the pile $P1$ decrease with increasing the distance between the tunnel axis and the beneath-piled building. The magnitude lateral deflection of pile $P1$ occurring at the depth of the tunnel axis was 3.7 mm, 2.8 mm, 2.3 mm, 1.8 mm 1.5 mm for the distance from the tunnel centreline to the beneath piled building of 2D, 3D, 4D, 5D, 6D respectively. The maximum vertical movements of pile P1 that occurred at the pile head were 28,7 mm, 25,9 mm, 24.3 mm, 23.6 mm and 23.2 mm for horizontal distance from tunnel centreline to the beneath piled building of 2D, 3D, 4D, 5D, and 6D respectively.
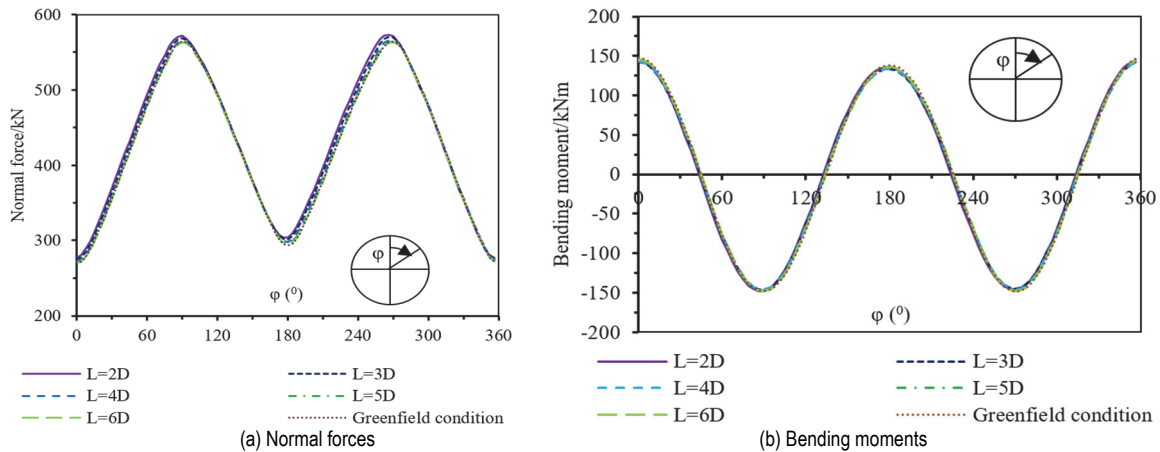

(a) Normal forces (b) Bending moments

Figure 11 The internal forces in the tunnel lining with varying distances from the tunnel centreline to the beneath-piled building L

The magnitudes of axial force and bending moment of the pile $P1$ decrease with increasing the lateral distance from the tunnel centreline to the beneath piled building (L) as shown in Fig. 10c and Fig 10d. At a lateral distance from the tunnel centreline to the beneath piled building $L = 2D$, the magnitude axial force of pile $P1$ occurring at the tunnel axis level has increased by 25.2% (319.4 kN to 399.8 kN) compared to that without tunnel case. The magnitude of the bending moment on pile $P1$ increased from 0.04 kNm to 1.108 kNm compared to that without tunnel case. Fig. 11a and Fig. 11b illustrate the distribution of axial forces and bending moments of the tunnel lining obtained by numerical analyses.

These results indicated the decrease in the distance from the tunnel centreline to the beneath-piled building due to the increase of the internal forces in the tunnel lining including normal forces. Compared with the greenfield condition, the maximum normal forces in the tunnel lining increased from 0.1% to 1.7% corresponding to the distance from the tunnel centreline to the beneath piled building decreased from 6D m to 2D m respectively (Fig. 11a). Compared with the greenfield condition, the maximum bending moments in the tunnel lining decreased from 0.6% to 0.3% when the distance from the tunnel to the beneath piled building decreased from 6D m to 2D m, respectively.

The axial forces and bending moments of the tunnel lining show very little change in magnitude compared to the greenfield values. The maximum normal forces and bending moments in tunnel lining are not significantly affected by the distance from the tunnel centreline to the beneath-piled building. By contrast, the axial force and bending moment of the pile are significantly impacted by that distance.
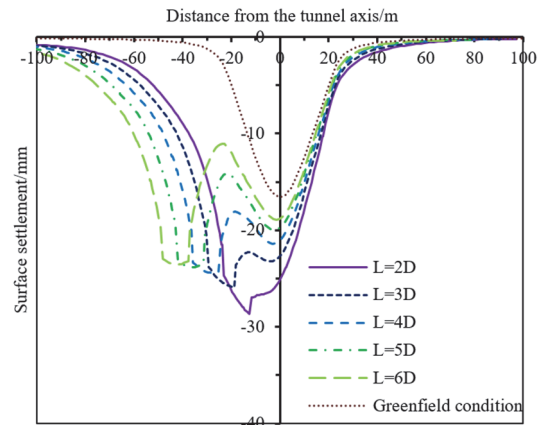

Figure 12 Ground surface settlement trough with varying distance from tunnel centreline to the beneath piled building L

The effects of the lateral distance from tunnel centreline to the beneath piled building (L) on ground surface settlement can be seen in Fig. 12. The values of the maximum ground surface settlement decrease with increasing lateral distance from tunnel centreline to the beneath piled building (L) and comparing them with green-field value, the maximum surface settlement is increased 72.9%, 56.2%, 47.2%, 43.6%, 42.1% for lateral distance from tunnel centreline to beneath piled building of 2D, 3D, 4D, 5D and 6D respectively. Fig. 13 and Fig. 14 show the effect of tunnel depth (Z) on internal forces in the tunnel lining and the pile $P1$ while keeping the horizontal distance from the tunnel centreline to the beneath-piled building, $L = 10$ m. In this study, a range of tunnel depth was considered ($0.5 Lp$, $0.75Lp$, $1.0Lp$, $1.25Lp$, and $1.5Lp$). The magnitudes of maximum axial force and bending moment in tunnel lining are significantly affected by the tunnel depth, but the magnitudes of axial force and bending moment in pile are not affected significantly by the tunnel

depth. Fig. 13 illustrates the effect of tunnel burial depth on response of the pile $P1$. The magnitude of the lateral deflection at pile head $P1$ is the largest when the tunnel burial depth is located at the pile tip $P1$ ($Z = Lp$), as shown in Fig. 13a. Fig. 12b illustrates the effect of tunnel burial depth on the vertical movement of pile $P1$, when comparing the maximum vertical movement of pile $P1$ with those found for the without tunnel case, the maximum vertical movement is increased by 20.1%, 38.6%, 52.1%, 63%, 64.2% for the tunnel burial depth of $0.5 Lp$, $0.75 Lp$, $1.0 Lp$, $1.25 Lp$ and $1.5 Lp$ respectively. These results found that the axial force of pile head $P1$ decreases with increasing the tunnel burial depth. The magnitude of the axial force of pile tip $P1$ is largest when the tunnel depth is located at the pile tip $P1$ ($Z = Lp$), as shown in Fig. 13c. Fig. 13d illustrates the effect of tunnel burial depth on the bending moment of pile $P1$; these results found that the bending moment of pile head $P1$ increases with increasing the tunnel burial depth.
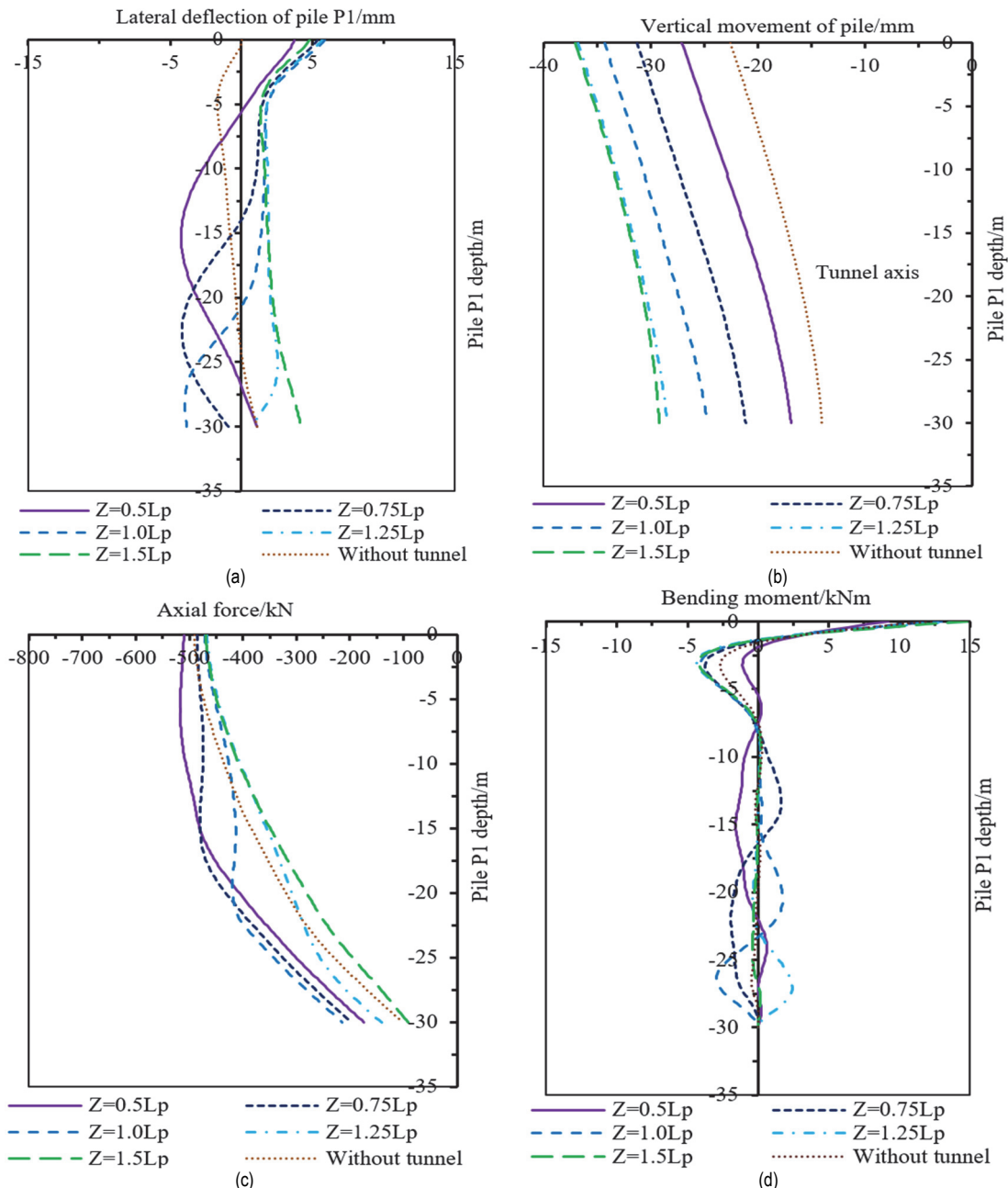

Figure 13 Distribution of (a) lateral deflection, (b) vertical movement, (c) axial force and (d) bending moment of pile $P1$ with varying tunnel depth Z
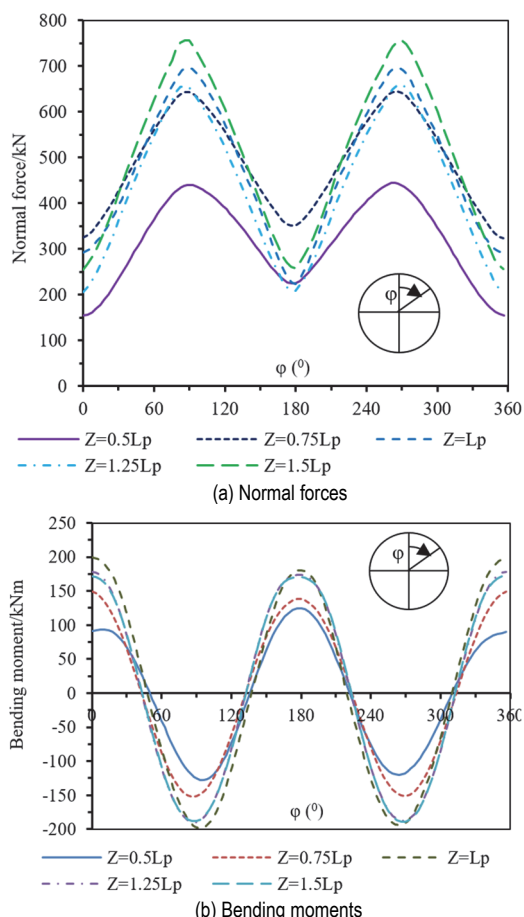
(a) Normal forces

(b) Bending moments

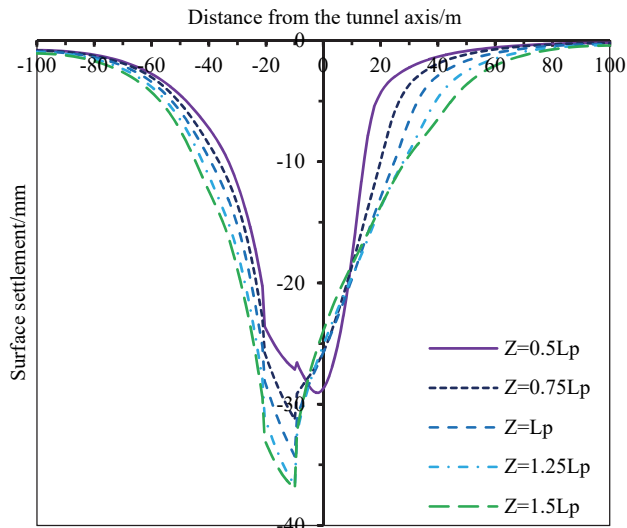**Figure 14** The internal forces in the tunnel lining with varying tunnel depth *Z*

Figure 15 Ground surface settlement trough with varying tunnel depth *Z*

Fig. 14 indicated that the magnitudes of normal forces and bending moments in the tunnel lining increase corresponding to the tunnel depth increase. The magnitude of maximum normal forces in the tunnel lining increases with burial depth from a value of 444.2 kN at a burial depth of $Z = 0.5$ *Lp* to 756.4 kN at a burial depth of $Z = 1.5$ *Lp*. The magnitude of the maximum bending moment in the tunnel lining increases from a value of 128.0 kNm at a burial depth of $Z = 0.5$ *Lp* to 189.0 kNm at a burial depth of $Z = 1.5$ *Lp*. The effect of tunnel depth on the surface settlement can be seen in Fig. 15. The magnitudes of surface ground settlements increase with depth, with

values of 29.1, 31.3, 34.3, 36.8 and 37.0 mm being found at a burial depth of 0.5 *Lp*, 0.75 *Lp*, 1.0 *Lp*, 1.25 *Lp* and 1.5 *Lp*. The magnitudes of surface ground settlements show a very small increase at a burial depth of $Z = 1.5$ *Lp*.

4 CONCLUSION

In this case study of Hanoi Metro line 03, 2D computational modeling has been performed to investigate the tunnel-soil-beneath piled building interaction. Two parameters of the tunnel burial depth and the distance from the tunnel centreline to the beneath piled building have been considered. The following conclusions are drawn from the analysis:

- The magnitude of the pile *P*1 response is greatest, which is the first pile loaded in the group, followed by piles in positions *P*2, *P*3 and *P*4.
- The distance from the tunnel axis to the beneath-piled building increases, and both the internal forces and displacements of the pile decrease. Whereas, these internal forces and displacements increase with greater tunnel burial depth.
- The magnitude of normal forces and bending moments in the tunnel lining increases as the tunnel burial depth increases, while normal forces increase and bending moments in the tunnel lining decrease when the distance from the tunnel axis to the beneath-piled building decreases.
- The distance from the tunnel axis to the beneath-piled building does not significantly affect the maximum axial forces and bending moments in the tunnel lining. However, it does significantly influence the internal forces and displacements of the pile.
- The tunnel burial depth has no significant effect on the internal forces and displacements of the pile, but it does have a significant impact on the maximum axial forces and bending moments in the tunnel lining.

The result obtained in this study can be used as a guide for tunnel construction in urban areas where nearby buildings are present.

5 REFERENCES

[1] Do, T. N., Dang, K. V., Pham, V. V., & Nguyen, Q. V. (2022). Prediction of surface settlement due to twin tunnelconstruction in soft ground of hanoi metro line 03. *International Journal of Geomate*, *22*(94). 66-72. https://doi.org/10.21660/2022.94.3209
[2] Do, T. N., Protosenya, A. G., & Vo, C. C. T. (2022). Prediction of ground surface settlement induced by twin tunnelling in urban areas (in Vietnamese). *Journal of Mining and Earth Sciences*, *63*(3a), 22-28. https://doi.org/10.46326/JMES.2022.63(3a).03
[3] Addenbrooke, T. I., Potts, D. M., & Puzrin, A. M. (1997). The influence of pre-failure soil stifiness on the numerical analysis of tunnel construction. *Geotechnique*, *47*(3), 693-712. https://doi.org/10.1680/geot.1997.47.3.693

[4] Attewell, P. B., Yeates, J. A., & Selby, A. R. (1986). Soil Movements Induced by Tunnelling and Their Effects on Pipelines and Structures. Blackie and Son Ltd, UK.

[5] Shi, J., Wang, J., Ji, X., Liu, H., & Lu., H. (2022). Three-dimensional numerical parametric study of tunneling effects on existing pipelines. *Geomechanics and Engineering*, *30*(4) 383-392.

[6] Marshall, A. M., Klar, A., & Mair, R. J. (2010). Tunneling beneath buried pipes: View of soil strain and its effect on pipeline behavior. *Journal of Geotechnical and Geoenvironmental Engineering*, *136*(12), 1664-1672. https://doi.org/10.1061/(ASCE)GT.1943-5606.0000390

[7] Marshall, A. M. & Mair, R. J. (2011). Tunneling beneath driven or jacked end-bearing piles in sand. *Canadian Geotechnical Journal*, *48*(12), 1757-1771. https://doi.org/10.1139/t11-067

[8] Hashash, F. Y., Dashti, M., Musgrove, S. M., Gillis, K. M., Walker, M., Ellison, M. K., & Basarah, S. M. (2018). Influence of tall buildings on seismic response of shallow underground structures. *Journal of Geotechnical and Geoenvironmental Engineering*, *144*(12), 04018097. https://doi.org/10.1061/(ASCE)GT.1943-5606.0001963

[9] Jeon, Y. & Lee, C. (2023). Analysis of pile group behaviour to adjacent tunnelling considering ground reinforcement conditions with assessment of stability of superstructures. *Geomechanics and Engineering*, *33*(5) 463-475.

[10] Lim, C. X., Jusoh, S. N., Lim, C. B., Abdullah, R. A., & Yunus, N. Z. M. (2023). Tunnel depth effect to pile in Tunnel's influence zone. *Tunnelling and Underground Space Technology*, *129*, 103298. https://doi.org/10.1016/j.pce.2022.103298

[11] Franziu, J. N., Potts, D. M., Addenbrooke, T. I., & Burland, J. B. (2004). The Influence of Building weight on Tunnelling-Induced Ground and Building Deformation. *Soils and Foundations*, *44*(1), 25-38. https://doi.org/10.3208/sandf.44.25

[12] O'Reilly, M. P. & New, B. M. (1982). Settlements above tunnels in the United Kingdom their magnitude and prediction. *Tunnelling '82, 3rd International Symposium., Inst of Mining and Metallurgy, London*, 173-181.

[13] Attewell, P. B. & Woodman, J. P. (1982). Predicting the dynamics of ground settlement and its derivitives caused by tunnelling in soil. *Ground Engineering*, *15*(7), 13-22. https://doi.org/10.1016/0148-9062(83)90142-0

[14] Mair, R. J., Taylor, R. N., & Burland, J. B. (1996). Prediction of ground movements and assessment of risk of building damage due to bored tunnelling. *Proceedings of International Symposium on Geotechnical Aspects of Underground Construction in Soft Ground. Mair & Taylor, London*, 713-718.

[15] Marshall, A. M. & Haji, T. (2015). An analytical study of tunnel-pile interaction. *Tunnelling and Underground Space Technology*, *45*, 43-51. https://doi.org/10.1016/j.tust.2014.09.001

[16] Franza, A. & Marshall, A. M. (2018). Centrifuge Modeling Study of the Response of Piled Structures to Tunneling. *Geotechnical and Geoenvironmental Engineering*, *144*(2), 04017109. https://doi.org/10.1061/(ASCE)GT.1943-5606.0001751

[17] Jing-chun, W., Da-peng, W., Wei-hong, H., & Xing, N. (2022). Life assessment of railway tunnel lining structure based on reliability theory. *Technical Gazette*, *29*(6), 1975-1982. https://doi.org/10.17559/TV-20221014070502

[18] Ng, C., Soomro, M., & Hong, Y. (2014). Three-dimensional centrifuge modelling of pile group responses to side-by-side twin tunnelling. *Tunnelling and Underground Space Technology*, *43*, 350-361. https://doi.org/10.1016/j.tust.2014.05.002

[19] Song, G. & Marshall, A. M. (2020). Centrifuge study on the influence of tunnel excavation on piles in sand. *Journal of Geotechnical and Geoenvironmental Engineering*, *146*(12), 04020129. https://doi.org/10.1061/(ASCE)GT.1943-5606.0002401

[20] Peck, R. (1969). Deep Excavations and Tunneling in Soft Ground. *Proc. 7th International Conference on Soil Mechanics and Foundation Engineering*, 225-281.

[21] Zuliang, Z., Chao, L., Xinrong, L., Yifei, F., & Ninghui, L. (2021). Analysis of ground surface settlement induced by the construction of mechanized twin tunnels in soil-rock mass mixed ground. *Tunnelling and Underground Space Technology*, *110*, 103746. https://doi.org/10.1016/j.tust.2020.103746

[22] Wang, Z., Yao, W., Cai, Y., Xu, B., Fu, Y., & Wei. G. (2019). Analysis of ground surface settlement induced by the construction of a large-diameter shallow-buried twin-tunnel in soft ground. *Tunnelling and Underground Space Technology*, *83*, 520-532. https://doi.org/10.1016/j.tust.2018.09.021

[23] Ayasrah, M., Qiu, H., Zhang, X., & Daddow, M. (2020). Prediction of Ground Settlement Induced by Slurry Shield Tunnelling in Granular Soils. *Civil Engineering Journal*, *6*(12), 2273-2289. https://doi.org/10.28991/cej-2020-03091617

[24] Systra, S. A. (2012). *Technical design statement, input data/volume I*. Package: Underground section Line and Stations, package number: hplmlp/cp-03. Project: Hanoi pilot light metro line 03. Hanoi metropolitan railway management board. Hanoi, Vietnam.

[25] Systra, S. A. (2012). *Geotechnical interpretative report underground section*. Package: underground section Line and Stations, package number: hplmlp/cp-03. Design report technical design, Project: Hanoi pilot light metro line 03. Hanoi metropolitan railway management board. Hanoi, Vietnam.

[26] Systra, S. A. (2012). *Preliminary building risk assessment report*. Package: Underground section Line and Stations package number: HPLMLP/CP-03. Design report technical design, Project: Hanoi pilot light metro line 03. Hanoi metropolitan railway management board. Hanoi, Vietnam.

[27] Xue, Y., Ranjith, P. G., Gao, F., Zhang, Z., & Wang, S. (2023). Experimental investigations on effects of gas pressure on mechanical behaviors and failure characteristic of coals. *Journal of Rock Mechanics and Geotechnical Engineering*, *15*(2), 412-428. https://doi.org/10.1016/j.jrmge.2022.05.013

[28] Xue, Y., Liu, S., Chai, J., Liu, J., Ranjith, P.G., Cai, C., Gao, F., & Bai, X. (2023). Effect of water-cooling shock on fracture initiation and morphology of high-temperature granite: Application of hydraulic fracturing to enhanced geothermal systems. *Applied Energy*, *337*, 120858. https://doi.org/10.1016/j.apenergy.2023.120858

Contact information:

Thai Ngoc DO, PhD
(Corresponding author)
Hanoi University of Mining and Geology,
Faculty of Civil Engineering,
No.18 Vien Street, Duc Thang Ward, Bac Tu Liem District, 100000, Hanoi,
Vietnam
E-mail: thaidongoc@gmail.com

Anatoliy Grigorevich PROTOSENYA, PhD, Professor
Saint-Petersburg Mining University,
Faculty of Civil Engineering,
No. 1, 21 line, 2. St. Petersburg, 199026, Russia
E-mail: Protosenya_AG@pers.spmi.ru

Nikita Andreevich BELYAKOV, PhD
Saint-Petersburg Mining University,
Faculty of Civil Engineering,
No. 1, 21 line, 2. St. Petersburg, 199026, Russia
E-mail: Belyakov_NA@pers.spmi.ru

Vi Van PHAM, PhD
(Corresponding author)
Hanoi University of Mining and Geology,
Faculty of Civil Engineering,
No.18 Vien Street, Duc Thang Ward, Bac Tu Liem District, 100000, Hanoi,
Vietnam
E-mail: phamvanvi0410@gmail.com

Quang Van NGUYEN, PhD
University of Transport Technology,
Faculty of Civil Engineering,
No.54 Trieu Khuc Street, Thanh Xuan Nam Ward, Thanh Xuan District, 100000,
Hanoi, Vietnam
E-mail: quangnv@utt.edu.vn